Iterative deblending with multiple constraints based on shaping regularization[a]

[a]Published in IEEE Geoscience and Remote Sensing Letters, 2015, doi: 10.1109/LGRS.2015.2463815

Yangkang Chen

ABSTRACT

It has been shown previously that blended simultaneous-source data can be successfully separated using an iterative seislet thresholding algorithm. In this paper, I combine the iterative seislet thresholding with the local orthogonalization technique via the shaping regularization framework. During the iterations, the deblended data and its blending noise section are not orthogonal to each other, indicating that the noise section contains significant coherent useful energy. Although the leakage of useful energy can be retrieved by updating the deblended data from the data misfit during many iterations, I propose to accelerate the retrieval of leakage energy using iterative orthogonalization. It is the first time that multiple constraints are applied in an underdetermined deblending problem and the new proposed framework can overcome the drawback of low-dimensionality constraint in the traditional 2D deblending problem. Simulated synthetic and field data examples show superior performance of the proposed approach.

KEYWORDS

Simultaneous sources, deblending, seislet thresholding, local orthogonalization, inversion with multiple constraints

INTRODUCTION

Modern seismic acquisition requires a high-density, wide-azimuth coverage for improving the subsurface illumination. Large acquisition systems require a highly efficient acquisition deployment. The principal purpose of simultaneous source acquisition is to accelerate the acquisition of a large-density seismic dataset, which can save acquisition cost and increase data quality. The benefits are compromised by the intense interference between different shots Beasley et al. (1998); Berkhout (2008); Abma and Yan (2009). Fig 1 shows a demonstration of the marine multi-source acquisition (two sources involved). The two sources shoot with a small random time dithering and thus will cause strong interference to the other source. The shooting time of each shot (shot schedules) are predefined in a separation-guided fashion and should be recorded correctly in order to formulated the inverse problem for source separation.

One approach to solve the problem caused by interference is by a first-separate and second-process strategy Beasley et al. (1998); Berkhout (2008); Abma and Yan (2009);

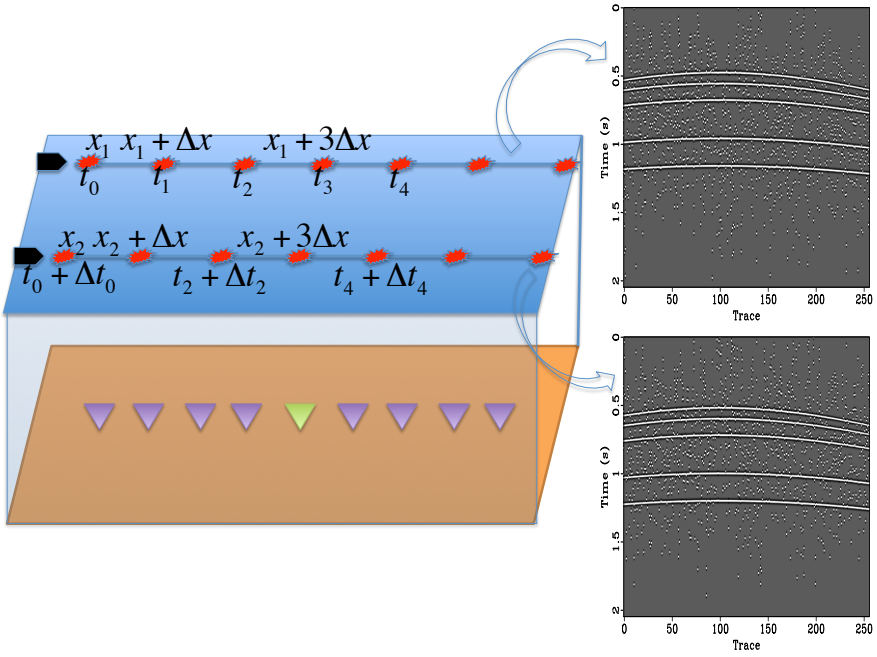

Figure 1: A demonstration of the marine two-source acquisition. .// demo

Chen et al. (2014a), which is also called deblending. Another way is by direct imaging and inversion of the blended data by attenuating the interference during the inversion process Berkhout (2008); Verschuur and Berkhout (2011); Xue et al. (2014); Chen et al. (2015).

There are generally two types of deblending approaches that have been investigated in the literature: (1) treating deblending as a noise filtering or attenuation problem Huo et al. (2012); Chen et al. (2014b); Chen (2014); Qu et al. (2015), (2) treating deblending as an inversion problem Abma et al. (2010); Chen et al. (2014a); Cheng and Sacchi (2015). Most of the filtering based approaches are based on median filtering (MF). Huo et al. (2012) used a multidirectional vector median filter after resorting the data into common midpoint gathers. Chen et al. (2014b) proposed using the common midpoint domain for deblending using a simple MF, because of the better coherency of useful signals than that in other domains and also because the useful near-offset events follow the hyperbolic assumption and can thus be flattened using normal moveout (NMO) correction. Chen (2014) proposed a type of MF with spatially varying window length. The space-varying median filter (SVMF) does not require the events to be flattened. For inversion based approaches, the ill-posed property of the inversion problem requires some constraint to regularize the inversion problem. Akerberg et al. (2008) used sparsity constraints in the Radon domain to regularize the inversion. Abma et al. (2010) proposed using $f-k$ domain sparsity as a constraint. Bagaini et al. (2012) compared two separation techniques for the dithered slip-sweep (DSS) data using the sparse inversion method and f-x predictive filtering Canales (1984); Chen and Ma (2014); Gan et al. (2015), and pointed out the advantage of the inversion methods over the filtering based approaches. In order to deal with the aliasing problem, Beasley et al. (2012) proposed the alternating projection method (APM), which chooses corrective projections to exploit data characteristics and appears to be less sensitive to aliasing than other approaches.

Currently, deblending is the crucial subject for obtaining a successful marine simultaneous-source acquisition. While the industry has obtained encouraging success in 3D deblending problem (e.g. OBN based 3D acquisition), the 2D deblending problem (e.g. marine towed-streamer acquisition) is still in trouble mainly because of the limited constraints that one can put onto the inversion problem. Chen et al. (2014a) proposed a general iterative deblending framework via shaping regularization Fomel (2007). The constraint for the ill-posed inversion problem is applied via the shaping operator which amounts to thresholding in the transformed domain. In this paper, I propose a new iterative deblending approach based on shaping regularization. Instead of simply enforcing the sparsity constraint in the sparse transform domain, I propose to use iterative orthogonalization to compensate the energy loss during the sparsity-constrained inversion. I iteratively threshold each deblended data in the seislet transform domain Fomel and Liu (2010) and orthogonalize the deblended data and blending interference in order to mitigate the energy loss during each iteration. The proposed approach differs from the conventional deblending approaches by applying multiple constraints based on the shaping regularization framework. I apply this approach to both synthetic and field data example and demonstrate its superior performance in obtaining more precise deblended results.

METHOD

Deblending via shaping regularization

The blending process can be summarized as the following equation:

$$\mathbf{d} = \Gamma \mathbf{m}, \tag{1}$$

where $\mathbf{d}$ is the blended data, Γ is the blending operator, and $\mathbf{m}$ is the unblended data. The formulation of Γ has been introduced in Mahdad (2012) in detail. When considered in time domain, Γ corresponds to blending different shot records onto one receiver record according to the shot schedules of different shots. Deblending amounts to inverting equation 1 and recovering $\mathbf{m}$ from $\mathbf{d}$.

Because of the ill-posed property of this problem, all inversion methods require some constraints.

Chen et al. (2014a) proposed a general iterative deblending framework via shaping regularization Fomel (2007, 2008). The iterative deblending is expressed as:

$$\mathbf{m}_{n+1} = \mathbf{S}[\mathbf{m}_n + \mathbf{B}[\mathbf{d} - \Gamma \mathbf{m}_n]], \tag{2}$$

where $\mathbf{S}$ is the shaping operator, which provides some constraints on the model, and $\mathbf{B}$ is the backward operator, which approximates the inverse of Γ. The shaping regularization framework offers us much freedom in constraining an under-determined problem by allowing different types of constraints. In this paper, the backward operator is simply chosen as $\lambda\Gamma^*$, where λ is a scale coefficient closely related with the blending fold, and Γ^* stands for the adjoint operator of Γ (or the pseudo-deblending operator). For example, λ can be optimally chosen as $1/2$ in a two-source dithering configuration Chen et al. (2014a); Mahdad (2012). In the next two sections, I will first introduce the conventional way for choosing the $\mathbf{S}$ and then propose a novel way for designing the $\mathbf{S}$.

Iterative seislet thresholding

When $\mathbf{S}=\mathbf{A}^{-1}\mathbf{T}_{\tau}\mathbf{A}$, the iterative framework refers to the iterative seislet thresholding:

$$\mathbf{m}_{n+1}=\mathbf{A}^{-1}\mathbf{T}_{\tau_n}\mathbf{A}[\mathbf{m}_n+\lambda\Gamma^*[\mathbf{d}-\Gamma\mathbf{m}_n]], \tag{3}$$

where $\mathbf{T}_{\tau_n}$ denotes a thresholding operator with a threshold τ_n, $\mathbf{A}$ and $\mathbf{A}^{-1}$ are a pair of forward and inverse seislet transforms.

$\mathbf{T}_{\tau}$ can be either a soft-thresholding operator:

$$\mathbf{T}^s_{\tau}(x)=\left\{\begin{array}{lll}(|x|-\tau)*sign(x) & \text{for} & |x|\geq\tau \\ 0 & \text{for} & |x|<\tau\end{array}\right. , \tag{4}$$

or a hard thresholding operator:

$$\mathbf{T}^h_{\tau}(x)=\left\{\begin{array}{lll}x & \text{for} & |x|\geq\tau \\ 0 & \text{for} & |x|<\tau\end{array}\right. . \tag{5}$$

In this paper, all the examples are based on soft thresholding. I iteratively decrease the threshold τ in the seislet domain during the iterations.

Extra constraint: iterative orthogonalization

Let

$$\tilde{\mathbf{m}}_n=\mathbf{A}^{-1}\mathbf{T}_{\tau_n}\mathbf{A}[\mathbf{m}_n+\lambda\Gamma^*[\mathbf{d}-\Gamma\mathbf{m}_n]], \tag{6}$$

where $\tilde{\mathbf{m}}_n$ denotes the deblended data after nth iteration. The blending noise section after nth iteration can be expressed as $\Gamma^*\mathbf{d}-\tilde{\mathbf{m}}_n$. During the iterations, the blending noise section will contain coherent signal. I propose to iteratively orthogonalize the deblended data and its corresponding noise section, using local signal-and-noise orthogonalization Chen and Fomel (2015). The orthogonalization problem can be expressed as a regularized inversion problem:

$$\min_{\mathbf{w}_n}\| \overbrace{\Gamma^*\mathbf{d}-\tilde{\mathbf{m}}_n}^{blending\quad noise} -\mathbf{w}_n\circ \overbrace{\tilde{\mathbf{m}}_n}^{deblended\quad signal} \|_2^2+\mathbf{R}(\mathbf{w}), \tag{7}$$

where $\mathbf{w}_n$ is the local orthogonalization weight (LOW), $\mathbf{a}\circ\mathbf{b}=diag(\mathbf{a})\mathbf{b}=diag(\mathbf{b})\mathbf{a}$, which denotes Hadamard (or Schur) product, and $diag(\cdot)$ denotes the diagonal matrix composed of an input vector. $\mathbf{R}$ denotes a smoothing regularization operator. When using equation 7, I assume that the signal and blending noise do not correlate with each other. The weighting vector $\mathbf{w}$ can be solved using shaping regularization Fomel (2007) with a local-smoothness constraint:

$$\mathbf{w}_n=[\lambda^2\mathbf{I}+\mathcal{T}(\mathbf{M}^T\mathbf{M}-\lambda^2\mathbf{I})]^{-1}\mathcal{T}\mathbf{M}^T(\Gamma^*\mathbf{d}-\tilde{\mathbf{m}}_n), \tag{8}$$

where $\mathcal{T}$ is a triangle smoothing operator, $\mathbf{M}=diag(\tilde{\mathbf{m}}_n)$, and λ is a scaling parameter. The orthogonalized deblended data can be expressed as:

$$\mathbf{m}_{n+1}=\mathbf{w}_n\circ\tilde{\mathbf{m}}_n+\tilde{\mathbf{m}}_n. \tag{9}$$

Combining equations 3 and 9 I obtain the following iterative framework using the proposed iterative orthogonalization and seislet thresholding:

$$\begin{aligned}\mathbf{m}_{n+1} = \mathbf{w}_n \circ \mathbf{A}^{-1}\mathbf{T}_{\tau_n}\mathbf{A}[\mathbf{m}_n + \lambda\Gamma^*[\mathbf{d} - \Gamma\mathbf{m}_n]]+ \\ \mathbf{A}^{-1}\mathbf{T}_{\tau_n}\mathbf{A}[\mathbf{m}_n + \lambda\Gamma^*[\mathbf{d} - \Gamma\mathbf{m}_n]].\end{aligned} \tag{10}$$

The iterative orthogonalization and seislet thresholding framework corresponds to an iterative shaping framework with two projections: thresholding in the seislet transform domain, and the orthogonalization between the deblended data and blending noise. It should be mentioned that the proposed approach can work robust in the case that inappropriate threshold parameters are selected because of an extra denoising compensation during each iteration that minimize the useful energy damages.

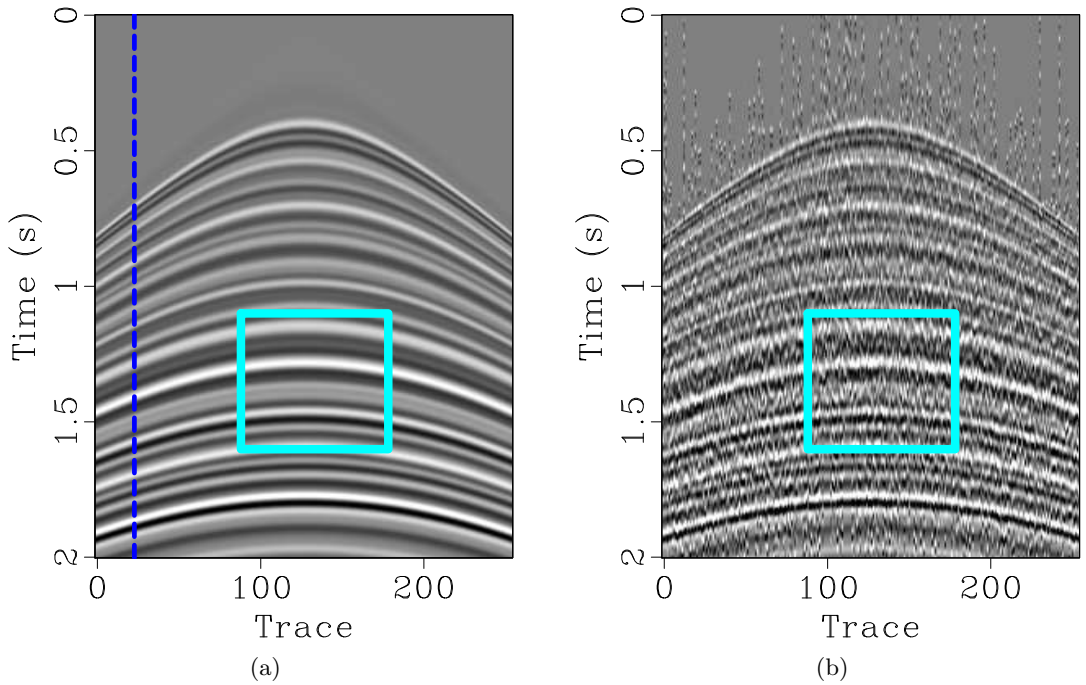

Figure 2: Simulated synthetic example. (a) Unblended data. (b) Blended data. hyper/ h1-1,hs-1

EXAMPLES

I first use a simulated synthetic example to demonstrate the performance of the proposed approach. I use the dithering approach following Chen et al. (2014a) to blend two sources in the common receiver domain. Fig 2a shows the unblended data. Fig 2b shows the blended data. I compare four approaches: $f-k$ thresholding, $f-x$ deconvolution, seislet thresholding, and the proposed approach. Both $f-k$ thresholding and seislet thresholding assumes that the seismic data is composed of local plane-wave components and is sparse in the transform domains Yuan et al. (2015). Fig 3 shows the deblended data using the four methods. The proposed approach and the seislet thresholding obtain significantly better results. Fig 4 shows the deblending error sections (difference between the deblended data

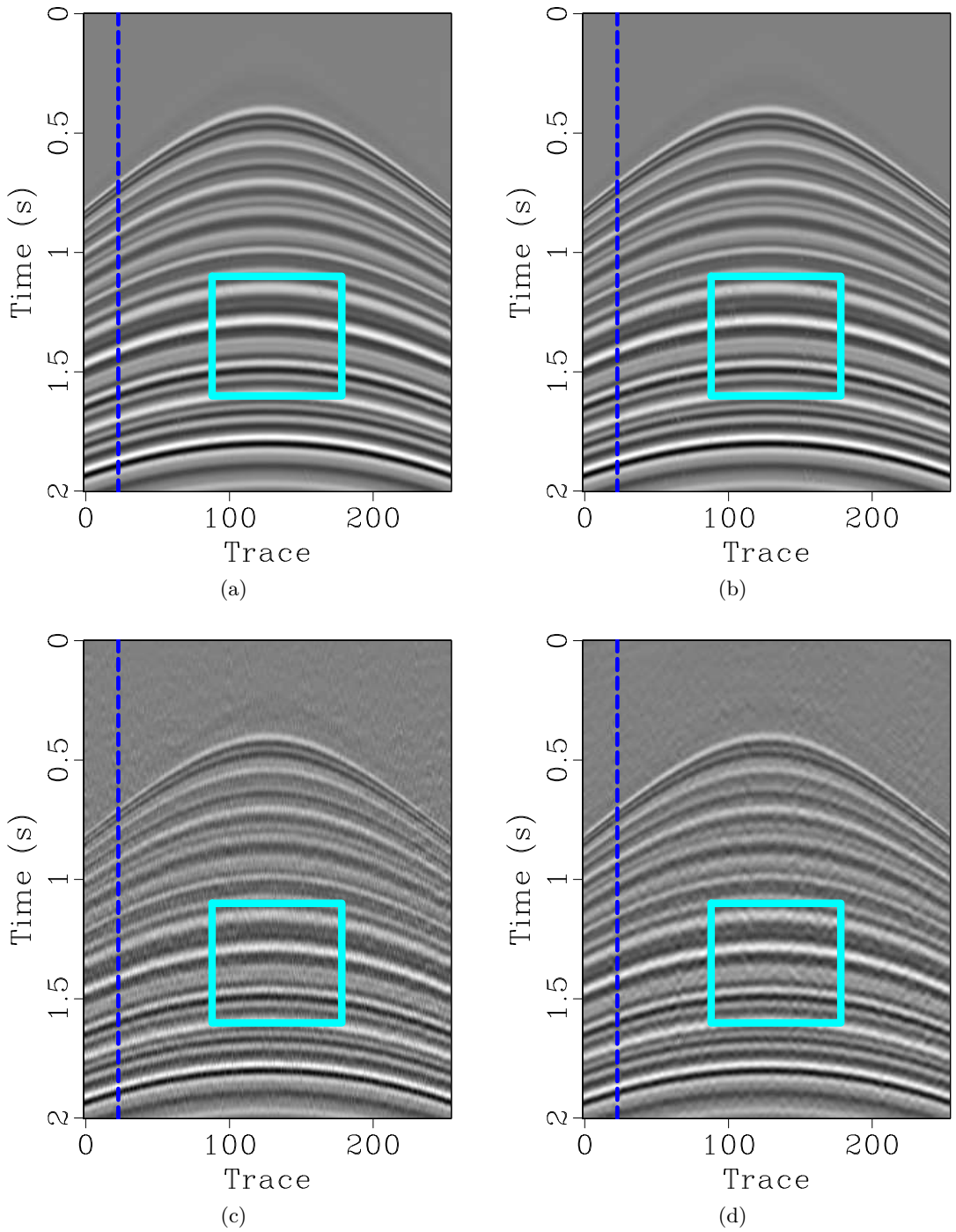

Figure 3: Simulated synthetic example. (a) Deblended data using the proposed approach. (b) Deblended data using seislet domain thresholding. (c) Deblended data using $f-k$ domain thresholding. (d) Deblended data using $f-x$ deconvolution. hyper/ hdbor1-1,hdbst1-1,hdbft1-1,hdbfx1-1

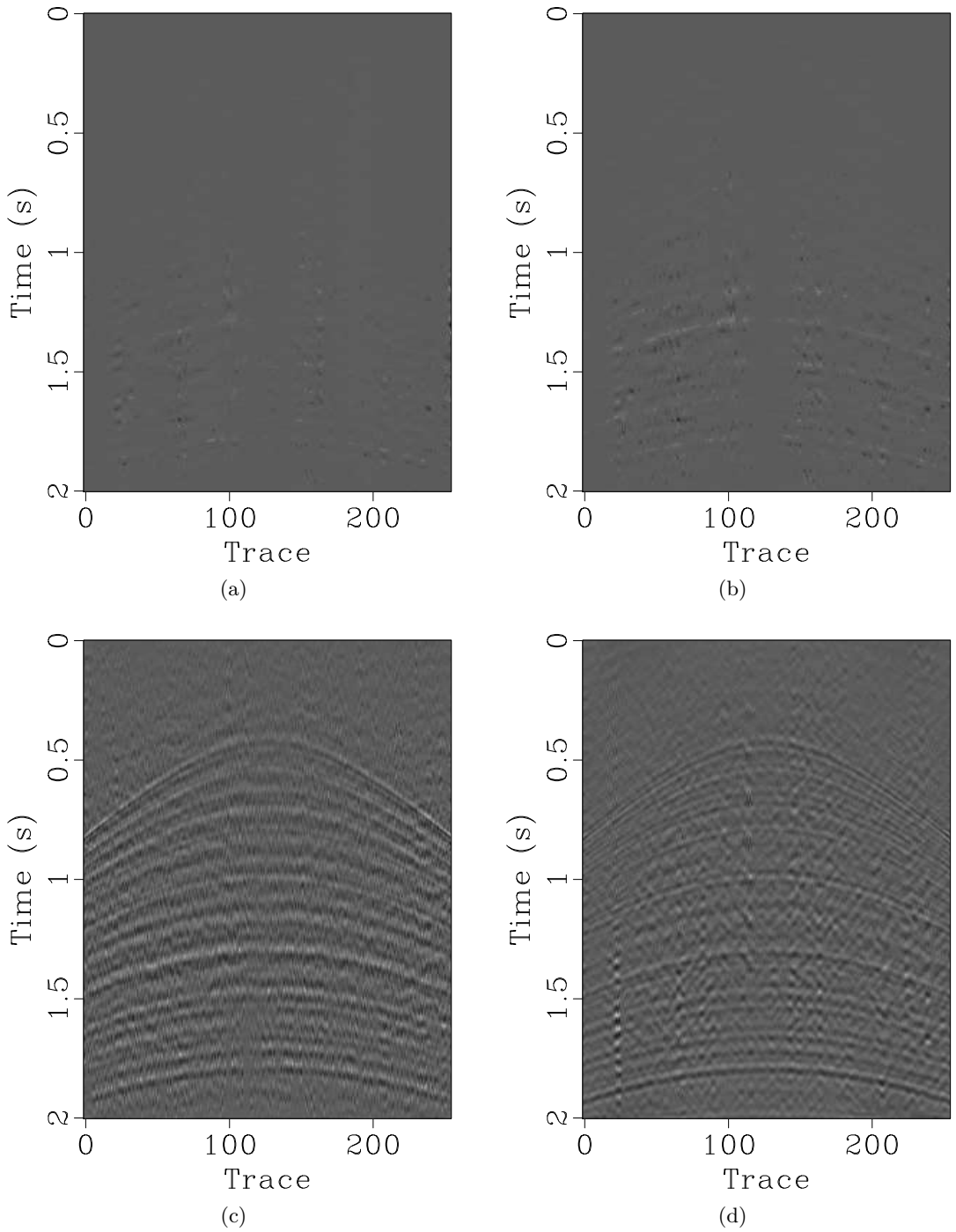

Figure 4: Simulated synthetic example. (a) Estimation error section using the proposed approach. (b) Estimation error section using seist domain thresholding. (c) Estimation error section using $f-k$ domain thresholding. (d) Estimation error section using $f-x$ deconvolution. hyper/ heor1,hest1,heft1,hefx1

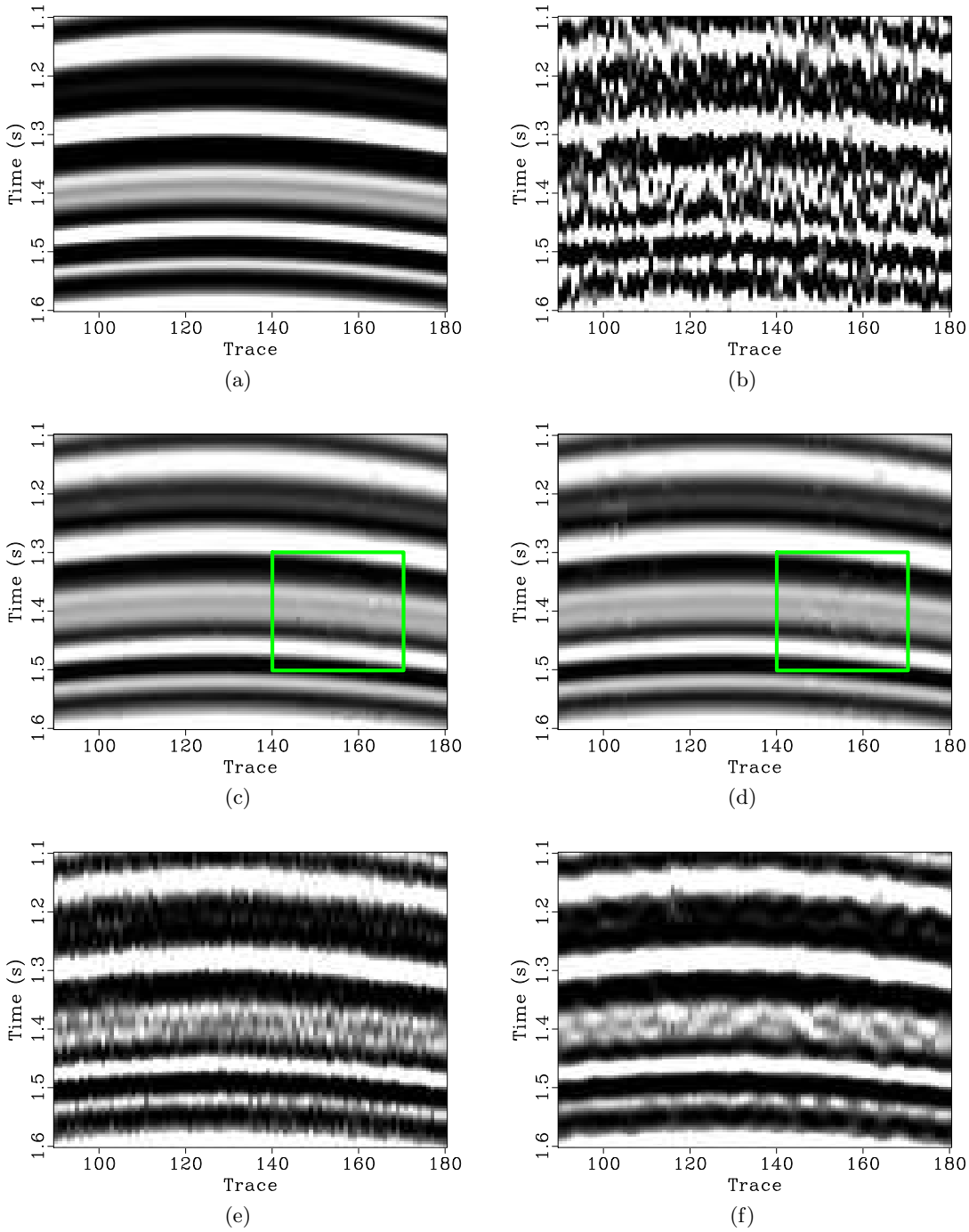

Figure 5: Zoomed section comparisons of the simulated synthetic example. (a) Unblended data. (b) Blended data. (c) Deblended data using the proposed approach. (d) Deblended data using seislet domain thresholding. (e) Deblended data using $f-k$ domain thresholding. (f) Deblended data using $f-x$ deconvolution. hyper/ h1-z,hs-z,hdbor1-z-0,hdbst1-z-0,hdbft1-z,hdbfx1-z

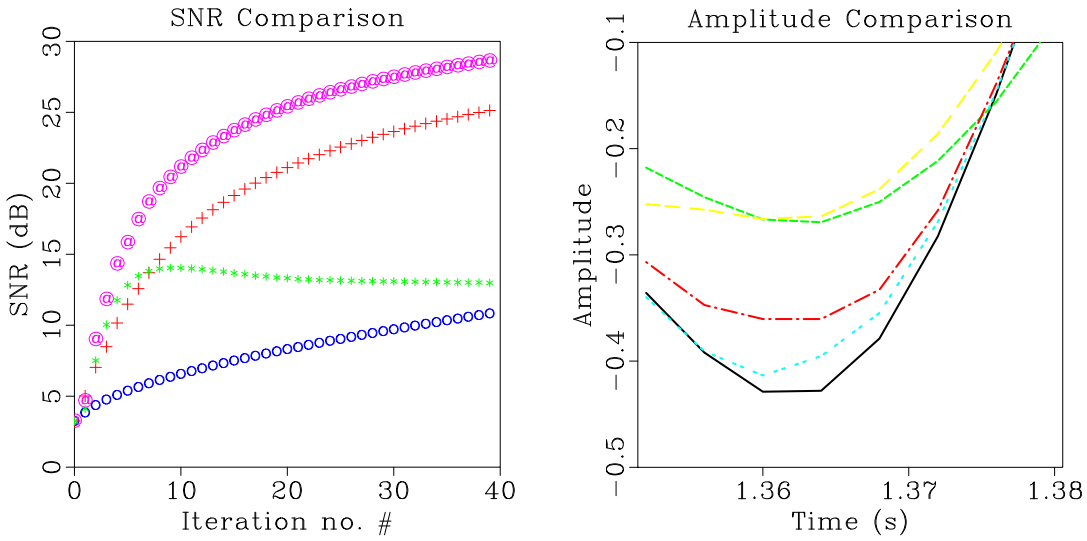

(a) (b)

Figure 6: (a) Comparison of signal-to-noise ratio of the simulated synthetic example. "@" refers to the proposed approach. "+" refers to seislet thresholding. "*" refers to $f-x$ deconvolution. "o" refers to $f-k$ thresholding. (b) Comparison of the amplitude between 1.35s and 1.38s of the 25th trace in the simulated synthetic data example. Black solid line denotes the unblended trace (true trace). Blue double dot line corresponds to the proposed approach. Red dot dash line corresponds to seislet thresholding. Green dash line corresponds to $f-k$ thresholding. Yellow long dash line corresponds to $f-x$ deconvolution. hyper/ hsnrsa,htc

and unblended data) using four different approaches. It confirms the fact that the proposed approach obtains the least deblending error, which is followed by the seislet thresholding. Fig 5 shows the zoomed sections from each figures in Figs 2 and 3. The zoomed regions are highlighted by the frameboxes in Figs 2 and 3. One can see the highlighted difference from the zoomed sections. Fig 6a shows the convergence diagrams in terms of the signal-to-noise ratio (SNR). The definition of SNR follows Yang et al. (2015):

$$SNR_n = 10 \log_{10} \frac{\|\mathbf{m}\|_2^2}{\|\mathbf{m} - \mathbf{m}_n\|_2^2}, \tag{11}$$

where $\mathbf{m}$ is the unblended data, SNR_n denotes the SNR after nth iteration. The convergence shows that while seislet thresholding can obtain very high SNR (around 24 dB), the proposed approach can obtain the highest SNR (above 30 dB). The proposed approach can also greatly accelerate the convergence. As shown in Fig 6a, it only takes around 15 iterations to achieve 25 dB, while the seislet thresholding takes more than 40 iterations to achieve a similar SNR.

Fig 6b shows the amplitude difference between 1.35s and 1.38s of the 25th trace in the simulated synthetic data example, as highlighted by the blue dash trace in Figs 2 and 3. The black solid line denotes the unblended trace (true trace). The blue double dot line corresponds to the proposed approach. The red dot dash line corresponds to seislet thresholding. The green dash line corresponds to $f - k$ thresholding. The yellow long dash line corresponds to $f - x$ deconvolution. The blue double dot line is the closest one to the black solid line. The red dot dash line is the second closest one to the black solid line. I conclude that, even though seislet thresholding can obtain a good deblending result, the proposed approach can further improve the performance. This superior performance is the same in all the profile. Here I only show a small portion of the trace in order to make the comparison clearer.

Fig 7 shows the deblending performance of the proposed approach on a simulated field data example. Figs 7a and 7d show the unblended and blended data, respectively. Figs 7b and 7c show the deblended data using seislet thresholding and the proposed approaches, respectively. Figs 7e and 7f show the estimation error sections using the two approaches. This example also shows that the proposed orthogonalization can improve the deblending performance of the traditional seislet thresholding.

I do not use local windows Yuan and Wang (2011) for all the aforementioned approaches and examples. Please note that when applied in local windows, all the approaches will work better. However, the seislet thresholding and the proposed approach does not need the local processing step and thus can be more convenient to implement. The limitation of the proposed approach is somewhat similar to the traditional iterative seislet thresholding approach, that is to say, the local slope need to be estimated correctly during the iterations and the data structure should not be too complicated. However, the orthogonalization can be combined with any existing iterative deblending approach and a combination of the orthogonalization strategy with other robust deblending approach can be a future investigation.

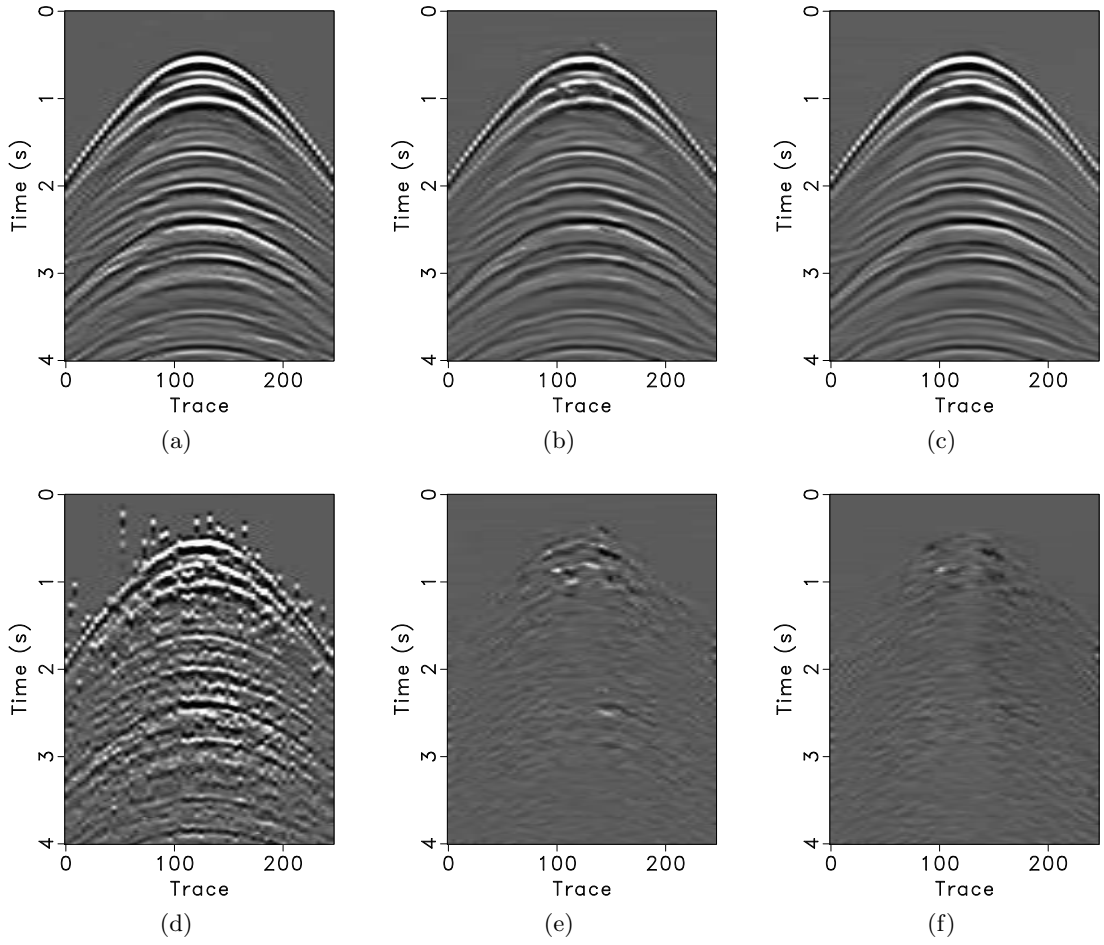

Figure 7: Simulated field data example. (a) Unblended data. (b) Deblended data using iterative seislet thresholding. (c) Deblended data using the proposed approach. (d) Blended data. (e) Estimation error using iterative seislet thresholding. (f) Estimation error using the proposed approach. .// field,slet,ortho,fields,slet-e,ortho-e

CONCLUSION

I have proposed a novel iterative deblending approach with multiple constraints: iterative orthogonalization and seislet thresholding. The principle of the proposed approach is to iteratively retrieve the leakage energy in the blending noise section after seislet thresholding during the iterations, using local orthogonalization. Because of the iterative orthogonalization, the data misfit during the iterations can be decreased significantly and thus the convergence can be accelerated. The final deblended performance can also be improved using the proposed approach, compared with that of seislet thresholding. Simulated synthetic and field data examples show a successful performance of the proposed approach.

ACKNOWLEDGEMENT

I would like to thank Ray Abma, Min Zhou, Sergey Fomel, Shuwei Gan, Shan Qu, Lele Zhang, Zhaoyu Jin, Jiang Yuan, Araz Mahdad, Josef Paffenholz, David Hays, Paul Docherty, and Craig Beasley for helpful discussions on the topic of deblending. I would specifically thank Sanyi Yuan, Sergey Fomel, Yanadet Sripanich, and three anonymous reviewers for grammar checks and constructive suggestions that help improve the manuscript greatly. The research is supported by Texas Consortium for Computational Seismology (TCCS).

REFERENCES

Abma, R. L., T. Manning, M. Tanis, J. Yu, and M. Foster, 2010, High quality separation of simultaneous sources by sparse inversion: 72nd Annual International Conference and Exhibition, EAGE, Extended Abstracts.

Abma, R. L., and J. Yan, 2009, Separating simultaneous sources by inversion: 71st Annual International Conference and Exhibition, EAGE, Extended Abstracts.

Akerberg, P., G. Hampson, J. Rickett, H. Martin, and J. Cole, 2008, Simultaneous source separation by sparse radon transform: 78th Annual International Meeting, SEG, Expanded Abstracts, 2801–2805.

Bagaini, C., M. Daly, and I. Moore, 2012, The acquisition and processing of dithered slip-sweep vibroseis data: Geophysical Prospecting, **60**, 618–639.

Beasley, C. J., R. E. Chambers, and Z. Jiang, 1998, A new look at simultaneous sources: 68th Annual International Meeting, SEG, Expanded Abstracts, 133–135.

Beasley, C. J., B. Dragoset, and A. Salama, 2012, A 3D simultaneous source field test processed using alternating projections: a new active separation method: Geophysical Prospecting, **60**, 591–601.

Berkhout, A. J., 2008, Changing the mindset in seismic data acquisition: The Leading Edge, **27**, 924–938.

Canales, L., 1984, Random noise reduction: SEG expanded abstracts:54th Annual international meeting, 525–527.

Chen, Y., 2014, Deblending using a space-varying median filter: Exploration Geophysics, doi:http://dx.doi.org/10.1071/EG14051.

Chen, Y., and S. Fomel, 2015, Random noise attenuation using local signal-and-noise orthogonalization: Geophysics, **80**, WD1–WD9.

Chen, Y., S. Fomel, and J. Hu, 2014a, Iterative deblending of simultaneous-source seismic data using seislet-domain shaping regularization: Geophysics, **79**, V179–V189.

Chen, Y., and J. Ma, 2014, Random noise attenuation by *f-x* empirical mode decomposition predictive filtering: Geophysics, **79**, V81–V91.

Chen, Y., J. Yuan, Z. Jin, K. Chen, and L. Zhang, 2014b, Deblending using normal moveout and median filtering in common-midpoint gathers: Journal of Geophysics and Engineering, **11**, 045012.

Chen, Y., J. Yuan, S. Zu, S. Qu, and S. Gan, 2015, Seismic imaging of simultaneous-source data using constrained least-squares reverse time migration: Journal of Applied Geophysics, **114**, 32–35.

Cheng, J., and M. Sacchi, 2015, Separation and reconstruction of simultaneous source data via iterative rank reduction: Geophysics, **80**, V57–V66.

Fomel, S., 2007, Shaping regularization in geophysical-estimation problems: Geophysics, **72**, R29–R36.

———, 2008, Nonlinear shapping regularization in geophysical inverse problems: 78th Annual International Meeting, SEG, Expanded Abstracts, 2046–2051.

Fomel, S., and Y. Liu, 2010, Seislet transform and seislet frame: Geophysics, **75**, V25–V38.

Gan, S., Y. Chen, S. Zu, S. Qu, and W. Zhong, 2015, Structure-oriented singular value decomposition for signal enhancement of seismic data: Journal of Geophysics and Engineering, **12**, 262–272.

Huo, S., Y. Luo, and P. G. Kelamis, 2012, Simultaneous sources separation via multidirectional vector-median filtering: Geophysics, **77**, V123–V131.

Mahdad, A., 2012, Deblending of seismic data: TU Delft, PhD thesis.

Qu, S., H. Zhou, Y. Chen, S. Yu, H. Zhang, J. Yuan, Y. Yang, and M. Qin, 2015, An effective method for reducing harmonic distortion in correlated vibroseis data: Journal of Applied Geophysics, **115**, 120–128.

Verschuur, D. J., and A. J. Berkhout, 2011, Seismic migration of blended shot records with surface-related multiple scattering: Geophysics, **76**, A7–A13.

Xue, Z., Y. Chen, S. Fomel, and J. Sun, 2014, Imaging incomplete data and simultaneous-source data using least-squares reverse-time migration with shaping regularization: 84th Annual International Meeting, SEG, Expanded Abstracts, 3991–3996.

Yang, W., R. Wang, Y. Chen, J. Wu, S. Qu, J. Yuan, and S. Gan, 2015, Application of spectral decomposition using regularized non-stationary autoregression to random noise attenuation: Journal of Geophysics and Engineering, **12**, 175–187.

Yuan, S., and S. Wang, 2011, A local f-x cadzow method for noise reduction of seismic data obtained in complex formations: Petroleum Science, **8**, 269–277.

Yuan, S., S. Wang, C. Luo, and Y. He, 2015, Simultaneous multitrace impedance inversion with transform-domain sparsity promotion: Geophysics, **80**, R71–R80.